Continental Shelf Research 31 (2011) 108–119

Contents lists available at ScienceDirect

Continental Shelf Research

journal homepage: www.elsevier.com/locate/csr

Research papers

Coastal and shelf circulation in the vicinity of Camamu Bay (14°S), Eastern Brazilian Shelf

F.N. Amorim [a,c,*,1], M. Cirano [b,c], I.D. Soares [d], C.A.D. Lentini [b,c]

[a] Instituto Oceanográfico da Universidade de São Paulo, Brazil
[b] Laboratório de Física Nuclear Aplicada, Instituto de Física, Universidade Federal da Bahia, Brazil
[c] GOAT—Grupo de Oceanografia Tropical, Brazil[1]
[d] Fundação Universidade Federal do Rio Grande, Brazil

ARTICLE INFO

Article history:
Received 1 March 2010
Received in revised form
8 September 2010
Accepted 22 November 2010
Available online 1 December 2010

Keywords:
Shelf currents
Seasonal variations
Wind-driven circulation
Tidally driven currents
Western boundary currents

ABSTRACT

The Camamu Bay (CMB) is located on the narrowest shelf along the South American coastline and close to the formation of two major Western Boundary Currents (WBC), the Brazil/North Brazil Current (BC/NBC). These WBC flow close to the shelf break/slope region and are expected to interact with the shelf currents due to the narrowness of the shelf. The shelf circulation is investigated in terms of current variability based on an original data set covering the 2002–2003 austral summer and the 2003 austral autumn. The Results show that the currents at the shelf are mainly wind driven, experiencing a complete reversal between seasons due to a similar change in the wind field. Currents at the inner-shelf have a polarized nature, with the alongshore velocity mostly driven by forcings at the sub-inertial frequency band and the cross-shore velocity mainly supra-inertially forced, with the tidal currents playing an important role at this direction. The contribution of the forcing mechanisms at the mid-shelf changes between seasons. During the summer, forcings in the two frequency bands are important to drive the currents with a similar contribution of the tidal currents. On the other hand, during the autumn season, the alongshore velocity is mostly driven by sub-inertial forcings and tidally driven currents still remain important in both directions. Moreover, during the autumn when the stratification is weaker, the response of the shelf currents to the wind forcing presents a barotropic signature. The meso-scale processes related to the WBC flowing at the shelf/slope region also affect the circulation within the shelf, which contribute to cause significant current reversals during the autumn season. Currents at the shelf-estuary connection are clearly supra-inertially forced with the tidal currents playing a key role in the generation of the along-channel velocities. The sub-inertial forcings at this location act mainly to drive the weak ebb currents which were highly correlated with both local and remote wind forcing during the summer season.

1. Introduction

The Camamu Bay (CMB), located along the Eastern Brazilian Shelf (EBS, 13°S–22°S; e.g. Knoppers, 1999), is an unique region because it not only hosts the narrowest straight continental shelf (17 km on average) along the South America Eastern Coast, but it is also placed in the region where the bifurcation of the South Equatorial Current (bSEC) takes place.

The bSEC originates the two shelf/slope Western Boundary Currents (WBC), the poleward Brazil Current (BC) and the equatorward North Brazil Current (NBC). Although its annual mean position occurs at 14°–16°S in the top 100 m (Stramma and England, 1999; Rodrigues et al., 2007), latitudinal excursions of the bSEC undergo a strong meridional wind seasonal cycle with southward displacements during austral winter followed by northward shifts during austral summer (Fig. 1). According to Rodrigues et al. (2007), these latitudinal excursions are mainly caused by the variability in the amplitude of the local wind stress curl due to the annual north-south displacements of the marine ITCZ. The bSEC latitudinal variability is strongest in the top 400 m, reaching its southernmost (northernmost) position ~17°S in July (~13°S in November).

The remote wind forcing is also an important driving mechanism in the local hydrodynamics. During austral winter, for instance, the trade winds are oriented in the east/southeast direction north of 20°S, whereas south of this latitude they are to the northeast. On the other hand, the trade winds convergence zone migrates to 12°S (Dominguez, 2006) during austral summer. This seasonal wind pattern change can be seen in the climatological wind roses for a grid point located in the central part of the EBS (Fig. 2).

Locally, the shelf hydrodynamics is also affected by the passage of cold atmospheric frontal systems. For example, Stech and

* Correspondence to: Cidade Universitária, Praça do Oceanográfico, 191, 05508-900, São Paulo, SP, Brazil.
E-mail addresses: fnamorim@usp.br, fnamorim@gmail.com (F.N. Amorim).
[1] www.goat.fis.ufba.br.

0278-4343/$ - see front matter © 2010 Elsevier Ltd. All rights reserved.
doi:10.1016/j.csr.2010.11.011

Lorenzzetti (1992) showed that the variability of the subtidal circulation of winter weakly stratified waters of the South Brazil Bight (SBB, 22°S–28°S) was highly dominated by those systems. During those events, the SBB showed a barotropic behavior with a quasi-geostrophic response to the local wind forcing. Likewise, as pointed out by Amorim et al. (2008) and Lima (2008), the passage of these frontal systems along the EBS is also capable of causing a complete reversal of the preferential flow.

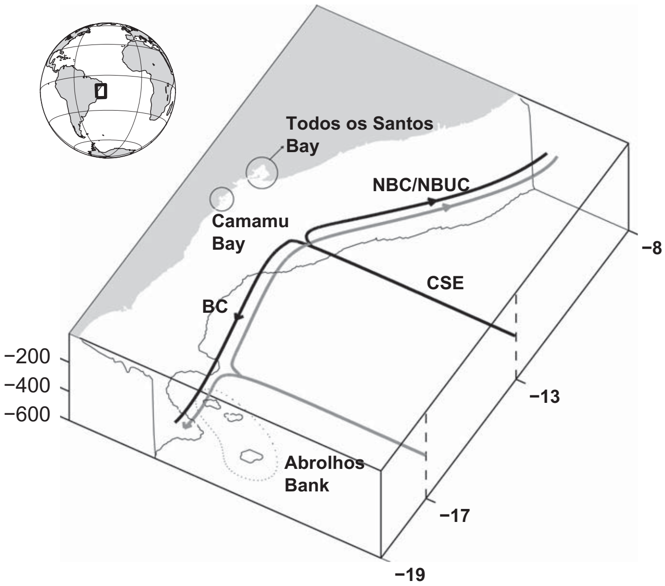

Fig. 1. Schematic seasonal variation of the WBC along the EBS based on southernmost (17°S in July) and northernmost position (13°S in November) of the SEC according to Rodrigues et al. (2007). The locations of the important ecosystems are also shown.

Furthermore, considering that the region of study is located in a narrow shelf with a minimum width of about 10 km and a shelf break around the 70 m isobath, it is expected that the dynamics of WBC at the shelf-break/slope region may exert a significant influence in the shelf hydrodynamics. Consequently, shelf currents can be subjected not only to meridional remote and local seasonal forcings, but also to transient meso-scale inputs. Our hypotheses is that the circulation within the CMB shelf is not only affected by the WBC dynamics, but it is also expected to be strongly influenced by the local and remote wind field, which may cause the reversal of the mean flow among seasons due to the seasonal wind pattern changes. The frequent arrival of atmospheric wintertime cold frontal systems can also change the direction of the preferential flow at the inner and mid shelves. Moreover, due to the proximity of an estuarine system, the inner and mid shelves are also expected to be under the influence of tidal currents. In addition to it is also important to point out that freshwater contributions to buoyancy-driven flows are meaningless due to the very low river discharges into the CMB, which do not change significantly between seasons (Table 1).

Ecologically speaking, the EBS is surrounded by important ecosystems such as the Todos os Santos Bay, the Abrolhos Bank and CMB (Fig. 1). Located in the central part of the EBS, CMB is still considered a pristine ecosystem and an important economic niche for the local fisheries. Moreover, in the last few years the CMB has been a constant target for oil and gas drilling activities (Hatje et al., 2008), which could affect the whole ecosystem in a case of an oil spillage.

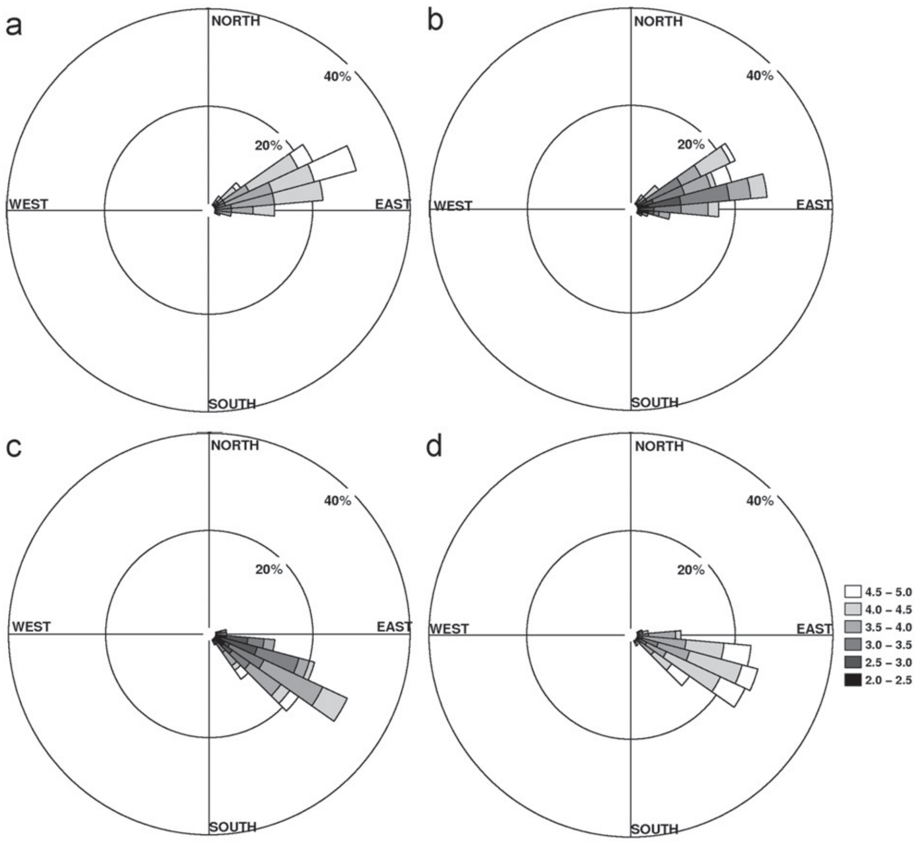

Fig. 2. Climatological wind roses (1976–2006) for a point located at the study region (see Fig. 3 for location) according to NCEP reanalysis. The wind roses presented are for the austral (a) spring, (b) summer, (c) autumn and (d) winter seasons.

Table 1
Mean discharge at CMB during the dry (August to February) and wet seasons (march to july), according to Amorim (2005).

River	Mean discharge ($m^3\ s^{-1}$)	
	Dry season	Wet season
Serinhaém	16.5	18.1
Igrapiúna	7.2	8.0
Pinaré	3.5	3.8
Sorojó	12.6	13.7
Maraú	11.2	12.1

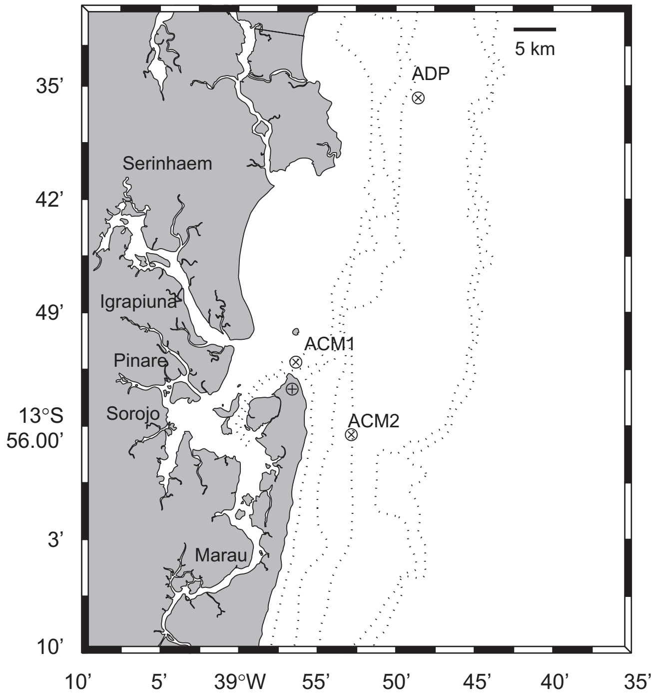

Fig. 3. Location map of the monitoring sites at the CMB shelf. Current time-series are obtained at ⊗ site and wind time-series at ⊕ site. The climatological wind roses derived from the NCEP reanalysis (Fig. 2) were obtained for the ADP site. The Serinhaém, Igrapiúna, Pinaré, Sorojó and Maraú rivers are the main tributaries. The bathymetry is indicated by the 10 m, 20 m, 30 m, 50 m and 200 m isobaths.

In spite of its hydrodynamical complexity and environmental value, there is still a lack of knowledge about the CMB coastal and shelf circulation. Therefore, the purpose of this manuscript is to provide for the first time a description of some of the most important driving mechanisms which control the shelf dynamics in the vicinity of CMB. In order to achieve this goal, current meter time series collected at 3 distinct locations (Fig. 3) during 2 different seasons are used to investigate the potential contribution of particular forcing mechanisms ranging from few hours (i.e., supra-inertial frequency) to several days (i.e., sub-inertial frequency). Thus, this work is organized as follows. Section 2 provides a description of the data and methods adopted here. Results of the main aspects of the seasonal, sub-inertial and supra-inertial circulation are shown in Section 3, followed by Section 4 which presents a brief discussion and the main conclusions of the results.

2. Data and methods

The data include coastal wind observations and ocean current measurements collected in three different locations: at the CMB adjacent inner and mid shelves and at the connection between the shelf and the estuarine system. Both the wind and the ocean current time series were registered in two distinct periods, which span the austral summer of year 2002/2003 and the austral autumn of year 2003. The later season is quite similar to the austral winter in terms of the preferential wind field as presented in Fig. 2, therefore the data are representative of two distinct seasons. Their dates and lengths are presented in Table 2 and the locations of the measurements are shown in Fig. 3. Although the data time series are not extensive, they represent the first current measurements of this kind for the region and were sufficient to the purpose of this work.

Table 2
Periods of the data measurements during the summer and autumn seasons. This Table is complemented with Fig. 3.

Local	Summer season	Autumn season
Current time series		
ACM1 site (15 m local depth)	2002/12/15–2003/02/02	2003/05/21–2003/06/25
ACM2 site (28 m local depth)	2002/12/15–2003/02/02	2003/05/21–2003/06/25
ADP site (42 m local depth)	2002/12/29–2003/01/21	2003/05/22–2003/06/27
Wind time series		
Ponta do Mutá	2002/12/16–2003/02/03	2003/05/24–2003/06/24

The wind time series were sampled by a *Wind Sentry RM Young* anemograph and the ocean current time series were registered by distinct instruments. At the entrance of the Bay (site ACM1 in Fig. 3) and at the inner-shelf site (ACM2 in Fig. 3) were used a *Falmouth Scientific 2D-ACM* acoustic current meters, positioned at 5 m from the surface. At the mid-shelf site (ADP in Fig. 3), the ocean current observations were taken with a *Sontek ADP* acoustic current meter profiler, which registered the currents between the 4–42 m depth. For this site, three different layers were chosen to be analyzed, the 5 m (which is coincident with the depth of the instruments at ACM1 and ACM2 sites), the 22 m and the 40 m layers. These depths are referred in the text as the surface, mid-depth and bottom layers, respectively.

The current and wind time series were decomposed and rotated in accordance with their axis of major variability, resulting in alongshore/channel (v) and cross-shore/channel (u) components. These components were analyzed in a three-fold procedure: (i) Basic statistics of the raw time-series; (ii) coherence analysis of the low-passed time-series and (iii) spectral decomposition and harmonic analysis of the high-passed time-series. The low-passed time series were obtained with the digital filter proposed by Walters and Heston (1982) with a cut-off period of 50 h, which represents the local inertial frequency. Power spectra density based on the Welch averaged periodogram method were performed to investigate the coherence between sub-inertial winds and currents, being all time-series detrended prior to computation and the 95% confidence limit observed the 8 degrees of freedom to the spectrum. For the current time-series collected throughout the water column (ADP site) an EOF analysis were also proceeded in order to investigate the contribution of the different modes of variability. The supra-inertial time-series were obtained applying the Walters and Heston (1982) filter with a cut-off period at the tidal frequency band (0.6–6 cpd) to avoid the high frequency variability associated with internal waves. The whole procedure was developed in MATLAB based on Emery and Thompson (1998).

3. Results

The mean aspects of the raw data are presented and the behavior of each vector component is investigated. In the next sessions the referred seasons are for the austral hemisphere.

3.1. Raw data

The wind behavior was in agreement with the climatological pattern (Fig. 2) blowing from N–NE during the summer season and from E–SE during the autumn season. The winds were mainly polarized at the alongshore direction, which presented similar magnitude and standard deviations between seasons (Table 3). Although both components of the wind presented part of their variability associated to the supra-inertial frequency band (at least 52% of the total variability), forcings at this frequency seems to be more relevant at the cross-shore direction, which presented standard deviations twice as the mean values (Table 3).

Currents at the shelf tended to follow the preferential wind direction, being mostly alongshore aligned and experiencing a complete reversal of the preferential flow due to the similar change in the wind orientation (Fig. 4 and Table 3). For both shelf sites the mean alongshore surface currents were more intense and less variable during the summer and presented high variability concentrated at the cross-shore direction, with standard deviations up to two orders of magnitude than the mean value.

At the mid-shelf ADP site the alongshore currents were marked by a significant reduction in their magnitude with depth (Fig. 4e–j, Table 3) during both seasons, although there was no change in orientation as a response of the Ekman veering. This behavior could

Table 3
Basic statistics of the alongshore/channel (v) and cross-shore/channel (u) current velocity and winds during the summer (s) and autumn (a) seasons, including the mean ($\overline{v}$,$\overline{u}$), standard deviations (σ_v,σ_u) and the percentage of variability ($\%var_v$, $\%var_u$) due to supra-inertial and tidal (in parenthesis) forcings. Positive values of v (u) at moorings ACM2 and ADP are northward (eastward) and at mooring ACM1 are off-shore (southward). Values are in cm s^{-1} for current velocity and m s^{-1} for winds.

	$\overline{v}$		$\overline{u}$		σ_v		σ_u		$\%var_v$		$\%var_u$	
	s	a	s	a	s	a	s	a	s	a	s	a
ACM1 (s)	4.4	2.7	−1.8	−2.7	36.4	33.9	9.5	6.8	99.6 (86.9)	97.5 (98.6)	77.7 (55.6)	87.5 (57.3)
ACM2 (s)	−20.7	13.4	−4.8	−3.5	8.5	13.6	5.6	4.7	28.5 (31.2)	12.9 (16.9)	65.6 (48.7)	60.0 (46.2)
(s)	−22.4	15.3	1.6	3.3	9.9	18.1	4.6	7.0	44.9 (48.8)	19.2 (33.8)	56.1 (44.7)	66.9 (41.3)
ADP (m)	−13.1	5.4	−0.5	−0.1	6.7	14.8	4.0	5.3	55.2 (64.5)	11.1 (18.7)	85.9 (60.6)	59.4 (35.3)
(b)	−4.7	1.5	−2.3	−0.9	6.4	9.6	3.6	5.3	48.5 (75.1)	17.9 (23.8)	66.4 (65.7)	64.9 (27.2)
Wind	−1.25	1.60	−0.13	0.96	1.60	1.75	1.37	1.60	52.2	60.7	86.3	66.5

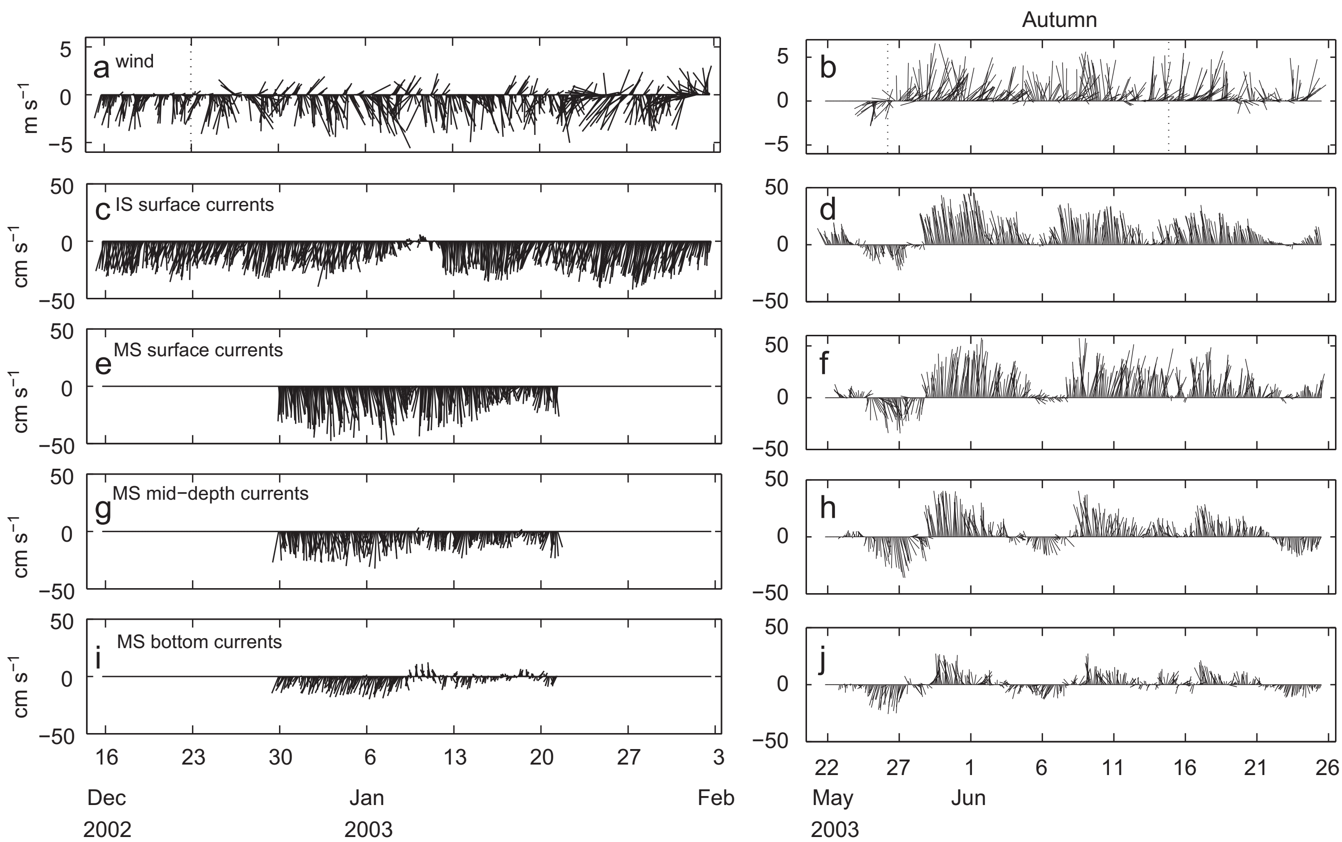

Fig. 4. Time series of the raw data (a, b) for wind, (c, d) inner-shelf surface currents and mid-shelf (e, f) surface, (g, h) mid-depth and (i, j) bottom currents, during summer and autumn seasons. IS and MS are related to the inner-shelf and mid-shelf sites (ACM2 and ADP in Fig. 3), respectively. Vertical dotted lines indicate cold-front passages.

be ascribed to weak winds blowing over a narrow shelf, as observed by Lentz and Winant (1986) at the Southern California Shelf. At the EBS, the passage of cold front systems is able to change the mean flow direction throughout the water column, as pointed out by Amorim et al. (2008). However, the current reversal along depth observed during the later May (Fig. 4f, h, and j) could not be ascribed to those systems, since it blows from S–SE. In addition, current reversals during the early and later June were also not related to the wind forcing, indicating that other important mechanism could affect the circulation at this region.

Although the currents at the shelf showed a similar behavior, their forcing mechanisms vary according to the seasons (Table 3). The surface alongshore currents at the ACM2 inner-shelf were mostly driven by sub-inertial forcings, responsible for up to 87% of the total variance, while the surface cross-shore currents were at least 60% supra-inertially forced. Tidal currents at this location acted mainly at the cross-shore direction, being responsible for almost 50% of the total variance in the supra-inertial frequency band. At the mid-shelf ADP site, the driving mechanisms did change between seasons. During the summer season the forcings at the two frequency bands acted similarly to drive the currents and the tidal currents played an important role in both alongshore and cross-shore direction, being responsible for at least 45% of the variability in the supra-inertial frequency band. During the autumn season the sub-inertial forcings were more important to drive the alongshore currents, which accounted for more than 81% of the total variance, while supra-inertial forcings represented more than 59% of the variance observed in the cross-shore currents. However, tidal driven currents still remained important at both directions of the flow.

Surface currents at the ACM1 shelf-estuary connection were clearly supra-inertially forced and mainly along-channel aligned. Tidal currents were responsible for at least 87% of along-channel variability and only up to 57% of the variability in cross-channel direction. The reduction of tidal forcing along this direction could be ascribed to the fact that cross-channel currents are more susceptible to variations caused by wind and lateral pressure gradients (Mantovanelli et al., 2004). Although there was a slightly change in the mean values of the along-channel surface current between the summer (4.4 cm s^{-1}) and autumn seasons (2.7 cm s^{-1}), they remained ebb oriented in both seasons (Table 3).

3.2. The sub-inertial band

The sub-inertial forcings were responsible for the weak surface currents at the ACM1 shelf-estuary connection, which remains ebb oriented throughout both seasons, except for the later June (Fig. 5). During the summer season, both components of the wind were effective in driving the along-channel currents ($\gamma^2 > 0.8$) and the out-of-phase correlation with the alongshore wind (with a 7 day period) reflected a coastal Ekman effect where a northern wind would drive an offshore flow (Fig. 6a). The in-phase correlation with the cross-shore winds in the 5–7 and 12 days period indicates that a wind blowing up estuary corresponds to a negative surface flow (Fig. 6b). During the autumn, the along-channel currents only presented a significant coherence ($\gamma^2 \sim 0.8$, not shown) with the cross-shore component of the wind and at periods of 7 days.

Currents at the adjacent continental shelf were more energetic in the alongshore direction and clearly correlated with the alongshore winds (Fig. 7). At the mid-shelf ADP site the alongshore velocity (solid lines) experienced an intense reduction toward the bottom, with no change in the direction of the preferential flow (Fig. 7 e–j) as a response of the Ekman veering. The cross-shore velocity (dashed lines) at this location showed an opposite orientation between surface and bottom depths, reflecting the Ekman dynamics (Fig. 7 e–j). An intense reversal of the currents was observed at the inner and mid shelves in the early and late June, which persisted for 4 days and was not related to the wind forcing. This behavior agrees with the dynamics of an anti-cyclonic eddy, as indicated by the absolute geostrophic velocities derived from Aviso (2010), which is more evident in the later June (Fig. 8).

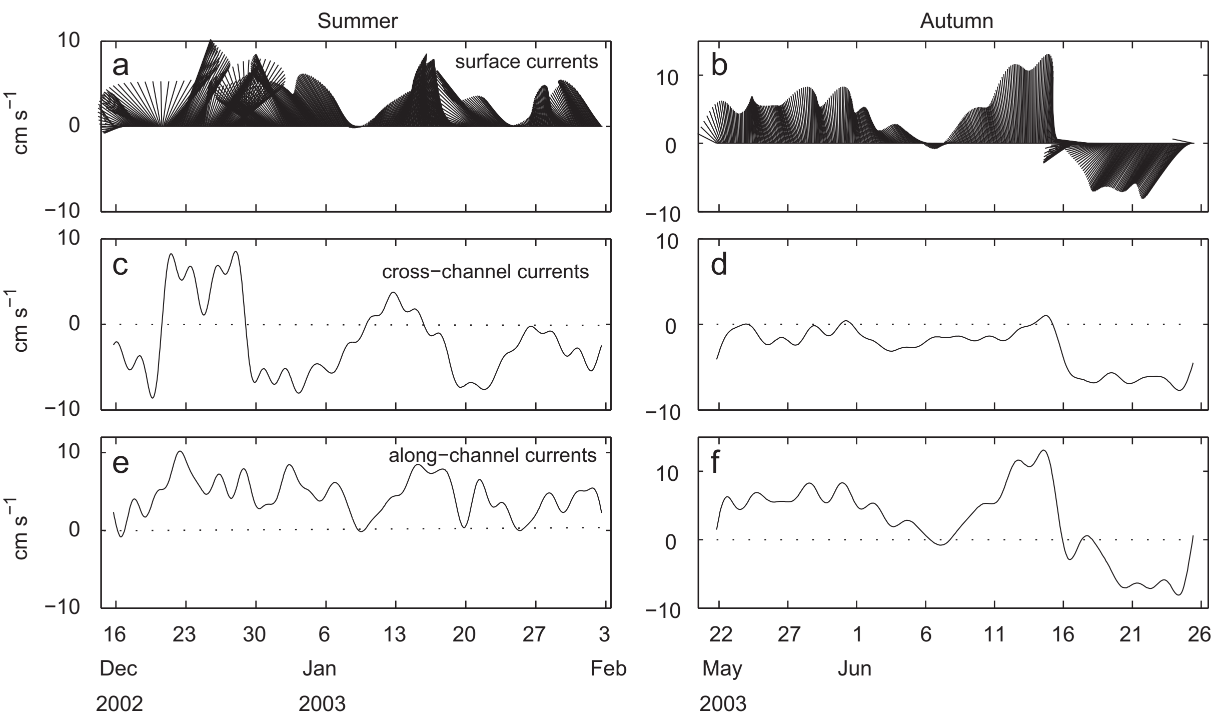

Fig. 5. Time series of the sub-inertial (a, b) surface current vectors at the ACM1 shelf-estuary connection and the associated (c, d) cross-channel and (e, f) along-channel velocity, during summer and autumn seasons. Positive along-channel (cross-channel) values are ebb (southeasterly) oriented.

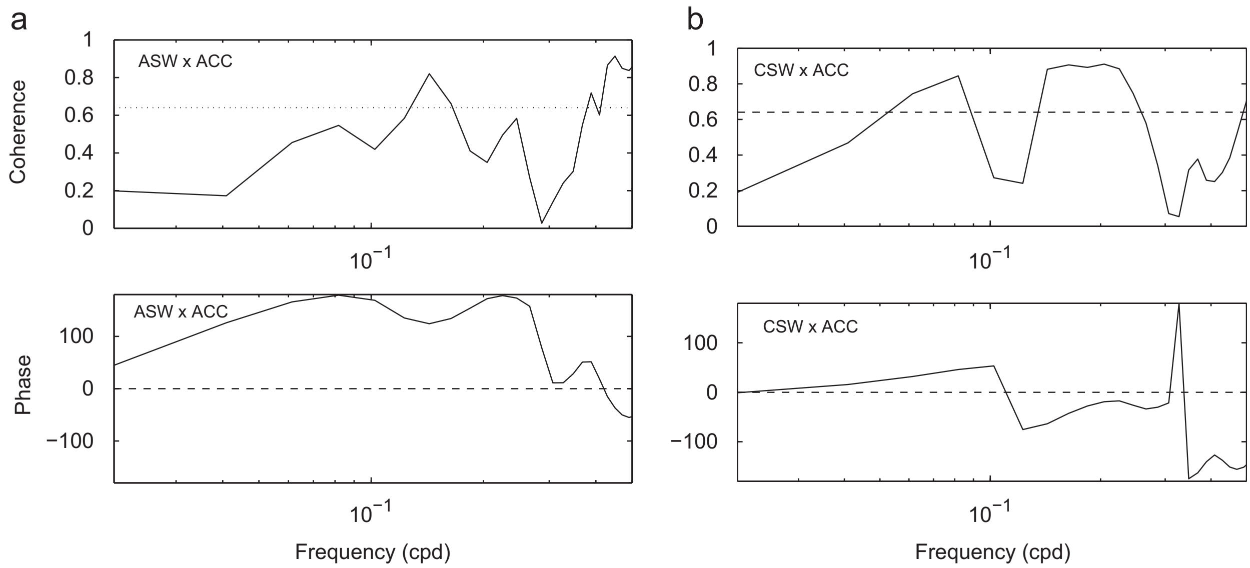

Fig. 6. Coherence squared and phase (angle) between the (a) alongshore (ASW) and (b) cross-shore wind (CSW) with the surface along-channel velocity (ACC) at the ACM1 shelf-estuary connection, during the summer season. Dotted line indicates the 95% confidence level.

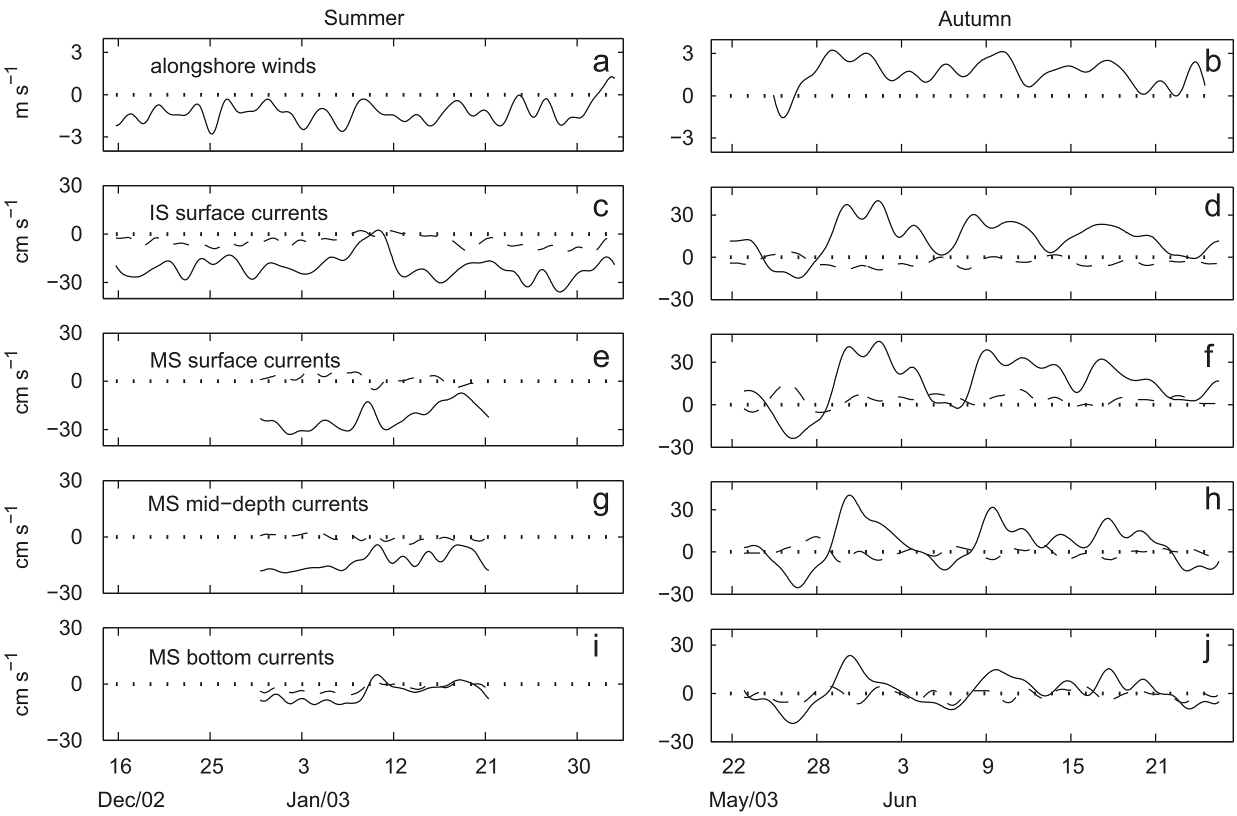

Fig. 7. Time series of sub-inertial (a, b) alongshore winds; (c, d) inner-shelf ACM2 alongshore and cross-shore surface velocity; mid-shelf ADP alongshore and cross-shore (e, f) surface, (g, h) mid-depth and (i, j) bottom velocity, during summer and autumn seasons. Solid (dashed) lines in Figures c–j represent the alongshore (cross-shore) velocity. IS and MS are related to the inner-shelf and mid-shelf sites, respectively.

Lagged cross-correlations between alongshore winds and currents at the shelf were computed (Fig. 9). Positive lags in this figure denote currents that lag the winds. Correlations at the inner-shelf ACM2 were only significant during the autumn season, when a peak of +0.8 occurs between wind and alongshore velocity with almost no lag (Fig. 9b), indicating southerly winds driving northward currents. The correlation peak of −0.48 with the cross-shore velocity (Fig. 9d) is less pronounced, indicating that these downwelling favorable winds are somehow correlated with the onshore flow.

At the mid-shelf ADP site, the correlation between alongshore winds and alongshore velocity was high (+0.6) during both seasons (Fig. 9e and f) and throughout the water column, characterizing a barotropic response of current to the wind forcing. However,

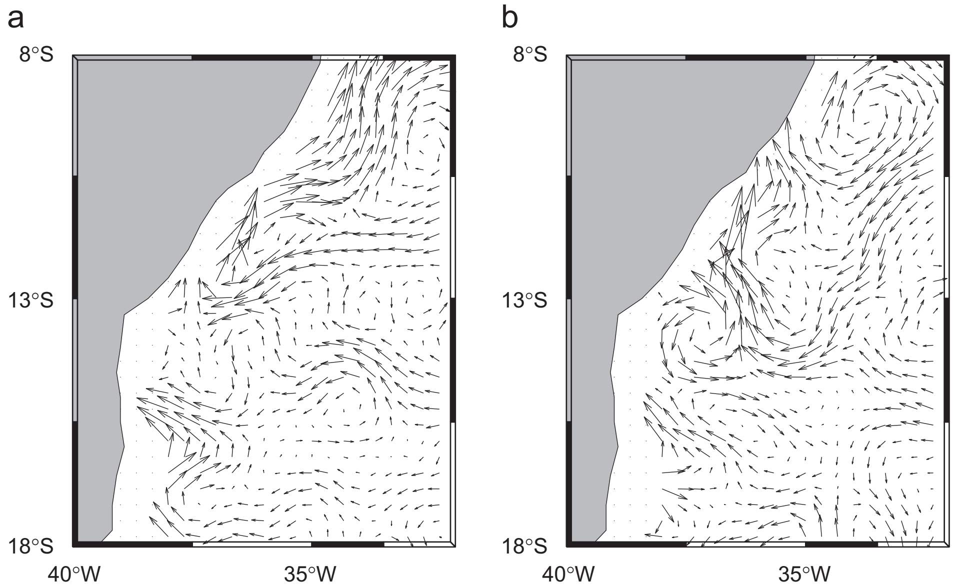

Fig. 8. Absolute geostrophic velocity derived from Aviso (2010). The events shown are a mean of the periods (a) 2003/06/4–11 and (b) 2003/06/21–28.

during the autumn, when the vertical stratification is weaker (e.g. Amorim et al., 2008), the response was higher (+0.8) with almost no lag along depth. The cross-shore velocity and alongshore winds presented an out-of-phase correlation at the surface and an in-phase correlation near the bottom with almost no lag (Fig. 9g and h), with a peak greater than ± 0.7 during the summer, reflecting the opposing surface and bottom Ekman layers.

Despite the strong stratification that occurs during the summer, the coherence ($\gamma^2 > 0.8$) between alongshore wind and alongshore velocity at the mid-shelf ADP showed a strong barotropic signal during both seasons (Fig. 10a and b), with an in-phase response at almost the entire sub-inertial band (0.05–0.25 cpd). During the autumn season, the results of Fig. 10b indicate a less pronounced lag between surface and bottom velocity. The cross-shore velocity (Fig. 10c and d), apart from the bottom velocity during the autumn, also presented a high coherence ($\gamma^2 > 0.8$) with the remote wind forcing. The phase relationship in Fig. 10c is an indicative of the existence of an upwelling system during the summer season.

The different modes of variability, accounted for the alongshore velocity, enhances the barotropic nature of flow at the mid-shelf ADP site (Table 4). Over 80% of the total variance during both seasons were accounted by the two first eigenfunctions, being at least 60% concentrated at the barotropic mode. The mean variance changes seasonally, with maximum energy concentrated in the autumn. The barotropic importance of the individual modes did not change significantly during seasons, but the baroclinic mode did. During the summer season the baroclinic mode was larger, accounting for 22% of the total variance, a response of the higher stratification observed during this season.

3.3. The supra-inertial band

The currents at the shelf-estuary connection ACM1(15 m water depth) were clearly supra-inertially forced and mainly along-channel aligned, as discussed in Section 3.1. Based on 25 tide components obtained by a harmonic analysis (Franco, 1988) of the supra-inertial currents at this location, we found that the semi-diurnal M_2 tidal component is the most important, followed by the S_2 tidal component, with amplitudes of 44.5 cm s^{-1} and 19.2 cm s^{-1}, respectively (Fig. 11). The two main diurnal components O_1 and K_1 (not shown) have amplitudes of 2.2 and 1.6 cm s^{-1}, respectively, and do not play an important role in the generation of these currents. Spectra estimates of the two components of the velocity show energetic peaks centered at the semi-diurnal frequency (Fig. 12a and b), with the along-channel velocity showing a broad peak centered at 24 h period, which correlates with the wind spectra (Fig. 12g and h). During the autumn, there were energetic peaks concentrated in a more gamma of the spectra (Fig. 12b), which can be ascribed to the strong wind variability during this season.

At the inner-shelf ACM2 site the ellipses of the two main semi-diurnal tidal components were mainly aligned in the cross-shore direction (Fig. 11) with a mean amplitude of the M_2 (S_2) component of 4 cm s^{-1} (1.8 cm s^{-1}). At the mid-shelf ADP site the ellipses were preferentially alongshore aligned, apart for the M_2 component during the summer, which enhances the finding that the tidal forcings act similarly at the two components of the flow during this season (e.g. Section 3.1). The mean surface tidal amplitudes at this portion of the shelf were 4 and 1.8 cm s^{-1} for the M_2 and S_2 components, respectively, with a slightly increase towards the bottom (dash-dotted ellipses).

The spectra of the two components of surface velocity at the shelf show broad peaks at the semi-diurnal frequency which correlate with peaks observed in the wind spectra (Fig. 12c–h). The energy associated with cross-shore variability is enhanced toward the coast (ACM2 site) during both seasons, being up to two orders of magnitude than the energy associated with the alongshore currents (Fig. 12c and d). However, at the mid-shelf ADP site there were peaks of energy concentrated at the 25 h period which are not observed at the inner-shelf site spectra, but correlates with the wind spectra (Fig. 12e–h). At this location, the energy associated with the alongshore velocity was higher during summer and similar to that on the cross-shore velocity during autumn, when the semi-diurnal wind coherence is significant.

At the mid-shelf ADP site where currents were recorded throughout the water column, the seasonal variability of the current profile structure was also investigated using EOF. In comparison with the sub-inertial variability (Table 4), there are necessary more modes of variability to account for the variance in the supra-inertial frequency band, and their nature change with the seasons (Table 5). The variance found during the summer for both alongshore and cross-shore velocity is concentrated in the first three modes, which accounted for more than 80% of the total variability. During the autumn season, when the stratification is

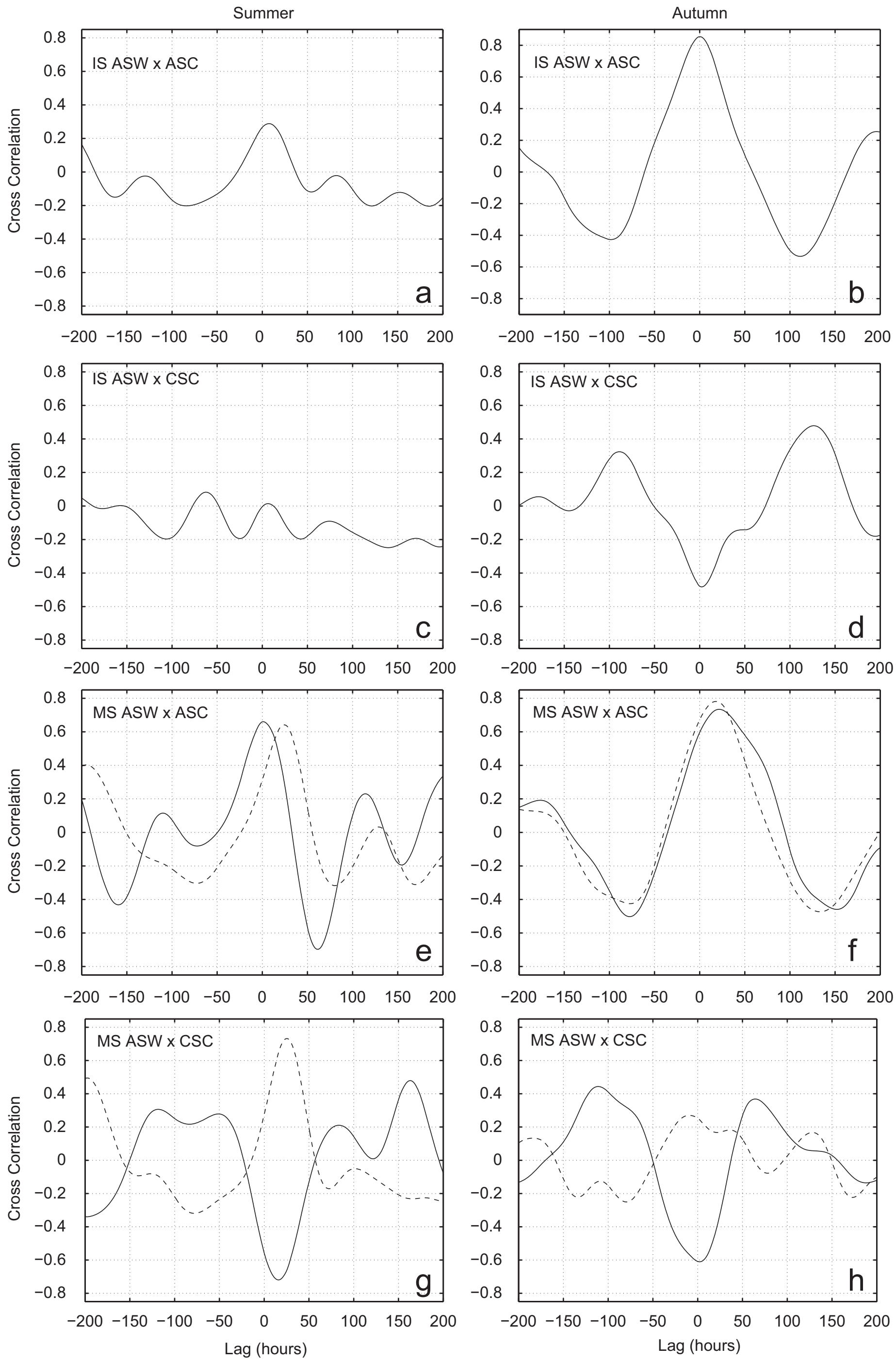

Fig. 9. Lagged cross-correlation functions between alongshore winds (ASW) versus (a, b) alongshore (ASC) and (c, d) cross-shore (CSC) velocity at inner-shelf ACM2 site; (e, f) alongshore and (g, h) cross-shore surface and bottom (dashed lines) velocity at mid-shelf ADP site, during summer and autumn seasons. IS and MS are related to the inner-shelf and mid-shelf sites, respectively.

weaker, the first three modes accounted for less than 70% of the total variance and the alongshore velocity variance reached its minimum value. The cross-shore variance did not change significantly between seasons.

4. Discussion and conclusions

The circulation of continental shelves has been the subject of many works in the last decades and there is a consensus that their dynamics varies according to the forcing mechanisms, the local topography and the width of the shelf. For instance, at the South Atlantic Bight and Southern Brazilian shelf, which are quite similar in terms of topography and forcing mechanisms, the inner shelf is buoyancy driven, whereas the combined effects of wind and Western Boundary Currents (WBC) are observed at the mid and outer-shelf (Lee et al., 1984; Soares and Moller, 2001). Conversely, the narrow Southern California Shelf shows no clear response to the Ekman dynamics and much of the alongshore current variability is unrelated to the wind forcing according to Lentz and Winant (1986).

In the present work, the circulation at Camamu Bay (CMB) continental shelf was investigated based on an original data set,

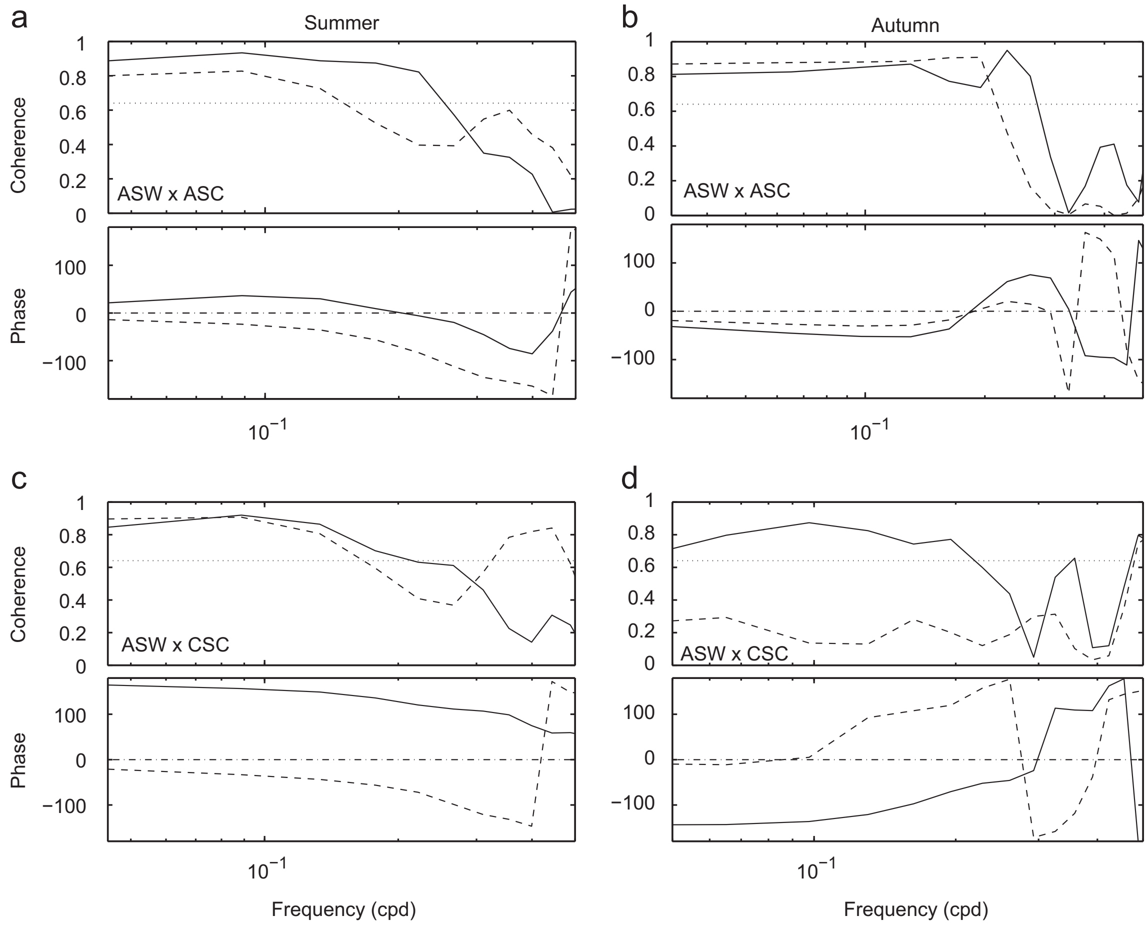

Fig. 10. Coherence squared and phase (angle) between the alongshore wind (ASW) and (a, b) alongshore (ASC) and (c, d) cross-shore (CSC) surface (solid line) and bottom (dashed line) velocity at the mid-shelf ADP site, during the summer and autumn seasons. Dotted line indicates the 95% confidence level.

Table 4
Mean sub-inertial alongshore velocity variance at the ADP site and the relative variance associated with each of the two largest eigenfunctions, during summer and autumn seasons.

Season	Variance ($cm^2 s^{-2}$)	Two largest eigenvectors	
Summer	26.0	0.60	0.22
Autumn	161.0	0.68	0.13

covering the 2002–2003 austral summer (late December 2002 until early February 2003) and the 2003 austral autumn (late May until June). The CMB shelf is a unique region, located at the vicinity of the South Equatorial Current bifurcation (bSEC) that originates two important WBC, the Brazil/North Brazil Currents (BC/NBC). It is also situated at the narrowest straight continental shelf along the South American Eastern Coast (17 km in average), the Eastern Brazilian Shelf (EBS). With such geographical configuration, the mean circulation is expected to have a close relationship with the features related to WBC. The CMB shelf is also located in a region under influence of the local and remote wind changes, passage of cold-front systems and tidal regime, resulting in very distinct autumn and summer scenarios. Moreover, the results showed that the circulation within the CMB shelf can be divided into three independent regions according to the forcing mechanisms.

At the shelf-estuary connection, the currents were clearly supra-inertially forced and their variability was mostly along-channel concentrated. The supra-inertial forcings were responsible for at least 97.5% of the total variance of the along-channel velocity, being up to 98.6% tidally driven. The cross-channel velocity was also driven by supra-inertial forcings, but their contribution in this component was less pronounced. Sub-inertial currents at this location were highly correlated with both the cross-shore and alongshore components of the wind during the summer season (Fig. 6), reflecting the effect of the remote and local wind forcing. During the autumn season, the along-channel velocity was highly correlated with the cross-shore winds at periods of 7 days, which may reflect the influence of the cold-front systems. The wind forcing seemed to be the main driving mechanism for the residual ebb currents at the shelf-estuary connection, since the buoyancy driven forcing are meaningless due to the low contribution of the continental drainage (Table 1).

At the shelf, the currents were clearly influenced by the wind forcing, following the direction of the prevailing winds and showing a complete reversal between the summer and autumn seasons (Fig. 4). During the summer season southward currents were driven by NE winds while during the autumn season northward currents were driven by SE winds. The contribution of the different forcing mechanisms in the generation of these currents though varies according to the seasons.

At the inner-shelf during both seasons, the alongshore velocity was mostly driven by sub-inertial forcings while the cross-shore velocity was mainly driven by supra-inertial forcings. In the supra-inertial band, the tidal currents were more important along the cross-shore axis. On the other hand, in the sub-inertial frequency band the alongshore winds were only significant in driving the alongshore velocity during the autumn season (Fig. 9b).

The mid-shelf currents were forced in the two frequency bands during the summer season, with tidally driven currents being

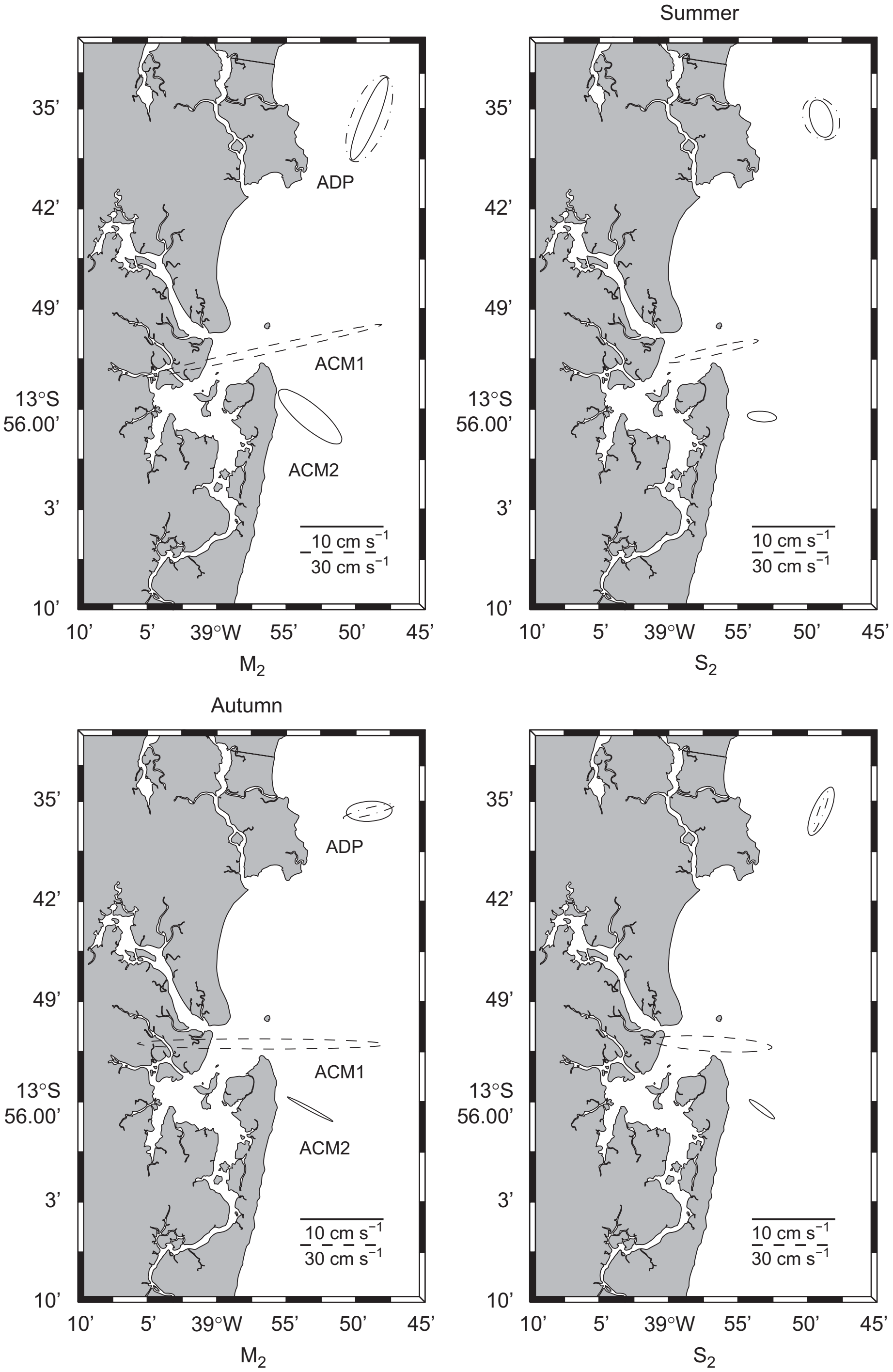

Fig. 11. Surface (~ 5 m depth) tidal ellipses of the two main tidal components at the shelf-estuary connection ACM1 site and the adjacent inner and mid-shelf sites (ACM2 and ADP). At the ADP site the bottom tidal ellipses (dash-dotted) are also presented. The dash-dotted line has the same scale of the solid line.

important in both the alongshore and cross-shore axis. During the autumn season, the sub-inertial forcings were more important in driving the alongshore velocity, although tidally driven currents still remained important in both directions. During both seasons, the sub-inertial alongshore surface and bottom flow were highly correlated with the alongshore winds (Fig. 9e and f), which somehow did not agree with the effect of the Ekman veering. However, the cross-shore surface velocity presented an out-of-phase correlation with the alongshore winds, while the near bottom velocity were in-phase (Fig. 9g and h), reflecting the dynamics of the two Ekman layers. Moreover, the high coherence and phase relationship between the cross-shore flow and alongshore winds at almost the entire sub-tidal band during the summer (Fig. 10c) indicates the presence of an upwelling system during this season.

The seasonal hydrographic changes also affected the sub-tidal current profile variability at the mid-shelf. The first two modes of variability accounted for almost the total alongshore current variance observed during both seasons with the dominance of a barotropic mode (Table 4). However, during the autumn season, when the mean variance was higher, the baroclinic mode was less

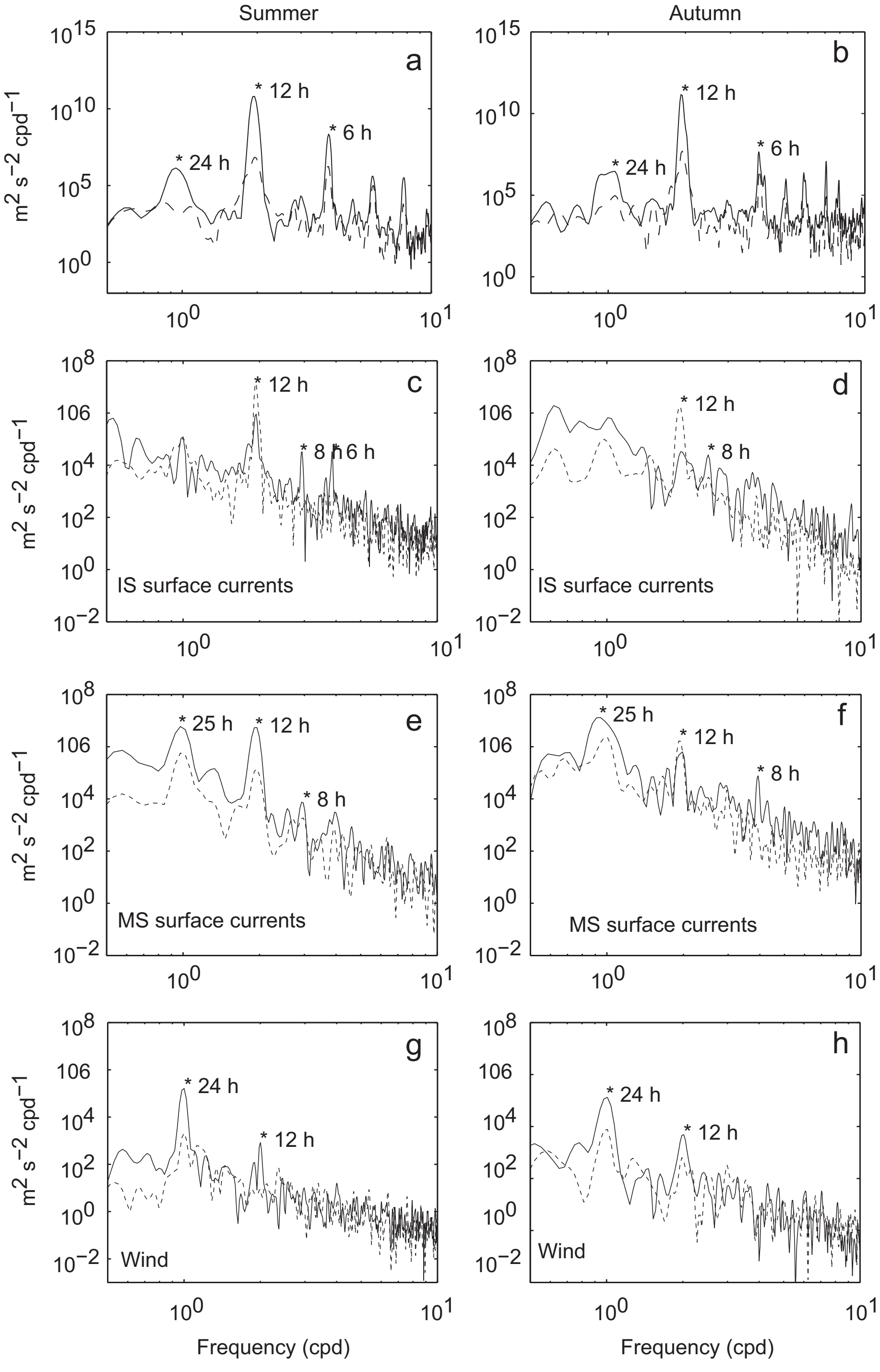

Fig. 12. Spectra of the surface alongshore/channel (solid line) and cross-shore/channel (dashed line) supra-inertial velocity at the (a, b) shelf-estuary connection ACM1, (c, d) inner-shelf ACM2 and (e, f) mid-shelf ADP sites during summer and autumn seasons. (g, h) The supra-inertial wind spectra. IS and MS are related to the inner-shelf and mid-shelf sites, respectively.

pronounced and the response of these currents to the wind forcing presented almost no lag throughout the water column (Fig. 9f), which could be a response to the weak stratification and relatively high turbulent vertical mixing, observed during this season. At the supra-inertial band, there were necessary more modes of variability to account for the total variance observed during the autumn season in comparison with the summer season (Table 5).

The meso-scale features related to the WBC, which flows closely to the shelf break and slope region, seemed to affect periodically the circulation within the CMB shelf. Significant current reversals, affecting the whole water column and observed during the autumn season (with a persistency of few days), were not related to the wind forcing (Fig. 7b, f, h, and j), but agreed with the dynamics associated with an anti-cyclonic eddy (Fig. 8). The influence of the WBC processes at the Brazilian shelf is well known (e.g. Campos et al., 1995; Soares and Moller, 2001), even in the region close to its formation, where it presents low current intensity (e.g. Soutelino et al., 2010). In a recent study based on hydrographic data close to the CMB shelf, Amorim et al. (2008) found an anomalous droop of the mixed layer depth during the wintertime, which the authors ascribed to be influenced by the dynamics associated to a cyclonic eddy related to the WBC activities.

Table 5
Mean supra-inertial variance for both components of the horizontal velocity at the ADP site and the relative variance associated with each of the three largest eigenfunctions, during summer and autumn seasons.

Season	Variance ($cm^2\ s^{-2}$)	Three largest eigenvectors		
Alongshore velocity				
Summer	22.0	0.47	0.24	0.13
Autumn	11.5	0.31	0.24	0.14
Cross-shore velocity				
Summer	5.8	0.37	0.26	0.19
Autumn	7.0	0.27	0.26	0.15

Based on the discussion presented above, some of the important findings resulted from this article were associated to the following points: (i) the tidal currents were the main forcing at the shelf-estuary connection; (ii) the currents at the inner-shelf showed a different response to the wind forcing between seasons and a polarized tidal current influence; (iii) the combined effects of wind forcing and tidal currents dominated the circulation at the mid-shelf; (iv) the meso-scale activities related to the WBC seemed to influence periodically the circulation at the shelf and (v) the whole system underwent a marked seasonal cycle in the large scale atmospheric circulation, resulting in very distinct autumn and summer scenarios. The last two points enhance the need to develop a monitoring program in the EBS to investigate the contribution of the South American WBC in controlling the coastal and shelf circulation in the vicinity of the CMB and in the EBS complex hydrodynamic system as a whole.

Acknowledgements

This work was supported by the Oceanographic Modeling and Research Network (REMO). Fabiola N. Amorim was supported by Brazilian scholarships from CAPES and REMO. Mauro Cirano was supported by a CNPq Research grant. We also thank El Paso Óleo e Gás do Brasil for providing all the data sets used in this manuscript.

References

Amorim, F.N., 2005. Caracterização Oceanográfica da Baía de Camamu e Adjacências e Mapeamento das Áreas de Risco à Derrames de Óleo. M.sc. Thesis, Universidade Federal da Bahia, Brazil, 194pp.

Amorim, F.N., Cirano, M., Soares, I.D., Campos, E.J.D., 2008. On the dynamics of Salvador Canyon, Bahia–Brazil (13S). In: Proceedings of the 27th International Conference on Offshore Mechanics and Artic Engineering, Estoril, Portugal, June 15–20.

Aviso, 2010. Absolute geostrophic velocities. NRT-Global-MADT 〈http://www.aviso.oceanobs.com〉.

Campos, E.J.D., Gonçalves, J.E., Ikeda, Y., 1995. Water mass characteristics and geostrophic circulation in the South Brazil bight—summer of 1991. J. Geophys. Res. 100 (9), 18,537–18,550.

Dominguez, J.M.L., 2006. The coastal zone of Brazil—an overview. J. Coast. Res. Sp. Iss. 39, 16–20.

Emery, W.J., Thomson, R.E., 1998. Data Analysis Methods in Physical Oceanography. Pergamon Press, Oxford.

Franco, A.S., 1988, Tides: fundamentals, analysis and prediction. São Paulo, Fundaç ão Centro Tecnológico e Hidráulica, 249pp.

Hatje, V., Barros, F., Magalhaes, W., Riatto, V.B., Amorim, F.N., Figueiredo, M.B., Spanó, S., Cirano, M., 2008. Trace metals and benthic macrofauna distributions in Camamu Bay, Brazil: sediment quality prior oil and gas exploration. Mar. Pollut. Bull. 56, 363–370.

Knoppers, B., Ekau, W., Figueiredo, A.G., 1999. The coast and shelf of east and northeast Brazil and material transport. Geo-Marine Letters 19, 171–178.

Lee, T.N., Ho, W.J., Kourafalou, V., Wang, J.D., 1984. Circulation on the continental shelf of the southeastern United States. Part I: subtidal response to wind and gulf stream forcing during winter. J. Phys. Oceanogr. 14 (6), 1001–1012.

Lentz, S.J., Winant, C.D., 1986. Subinertial currents on the southern California shelf. J. Phys. Oceanogr. 16 (11), 1737–1750.

Lima, J.B., 2008. Caracterização Oceanográfica da Plataforma Continental na Região sob Influência dos Emissários Submarinos da Cetrel e Millennium. Monografia submetida para o curso de Bacharel em Ocenografia, Universidade Federal da Bahia, UFBA, 55pp.

Mantovanelli, A., Marone, E., Silva, E.T., Lautert, L.F., Klingenfuss, M.S., Prata, V.P., Noernberg, M.A., Knoppers, B.A., Angulo, R.J., 2004. Combined tidal velocity and duration asymmetries as a determinant of water transport and residual flow in Paranaguá Bay estuary. Est. Coast. Shelf Sci. 59 (4), 523–537.

NCEP—National Center of Environmental Prediction Reanalysis Data. National Oceanic and Atmospheric Administration, Cooperative Institute for Research in Environmental Sciences (NOAA-CIRES). Climate Diagnostics 〈http://www.cdc.noaa.gov/cdc/data.ncep.reanalysis.html〉.

Rodrigues, R.R., Rothstein, L.M., Wimbush, M., 2007. Seasonal variability of the South Equatorial Current bifurcation in the Atlantic Ocean: a numerical study. J. Phys. Oceanogr. 37 (1), 16–30.

Stech, J.L., Lorenzzetti, J.A., 1992. The response of the South Brazil Bight to the passage of wintertime cold fronts. J. Geophys. Res. 97 (C6), 9507–9520.

Stramma, L., England, M., 1999. On the water masses and mean circulation of the South Atlantic current. J. Phys. Oceanogr. 20, 846–859.

Soares, I.D., Moller Jr., O., 2001. Low-frequency and water mass spacial distribution on the Southern Brazilian shelf. Cont. Shelf Res. 21, 1785–1814.

Soutelino, R.G., Silveira, I.C.A., Gangopadhyay, A., Miranda, J.A., 2010. Is there an Eddy-dominated Brazil Current North of 20° S? In: Proceedings of the Eos Trans. AGU, Meet. Am. Suppl., Foz do Igassu, Brazil, 91(26)OS23A-10, August 8–12.

Walters, R.A., Heston, C., 1982. Removing tidal-period variations from time-series data using low-pass digital filters. J. Phys. Oceanogr. 12 (1), 112–115.